IEEE Photonics Journal
An IEEE Photonics Society Publication

Open Access

Optimization of Nonlinear Compensation in a High-Energy Femtosecond Fiber CPA System by Negative TOD Fiber

Volume 9, Number 2, April 2017

Huanyu Song
Bowen Liu
Liang Wen
Chingyue Wang
Minglie Hu

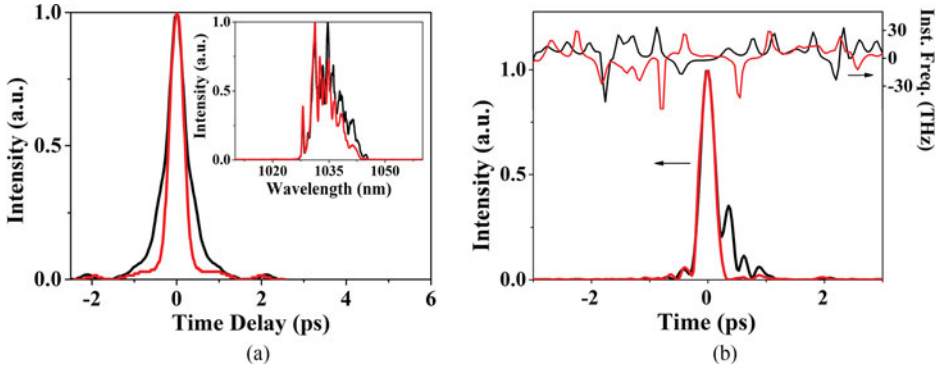

DOI: 10.1109/JPHOT.2017.2681704
1943-0655 © 2017 IEEE

Optimization of Nonlinear Compensation in a High-Energy Femtosecond Fiber CPA System by Negative TOD Fiber

Huanyu Song, Bowen Liu, Liang Wen, Chingyue Wang, and Minglie Hu

Ultrafast Laser Laboratory, Key Laboratory of Opto-Electronic Information Technical Science of Ministry of Education, School of Precision Instruments and Opto-Electronics Engineering, Tianjin University, Tianjin 300072, China

DOI:10.1109/JPHOT.2017.2681704

Manuscript received January 5, 2017; revised March 7, 2017; accepted March 9, 2017. Date of publication March 13, 2017; date of current version March 29, 2017. This work was supported in part by the National Natural Science Foundation of China under Grant 61227010, Grant 61535009, and Grant 61205131; in part by the Tianjin Research Program of Application Foundation and Advanced Technology under Grant 14JCQNJC02000; and in part by the Program for Changjiang Scholars and Innovative Research Team in University under Grant IRT13033. Corresponding authors: B. Liu and M. Hu (e-mail: bwliu@tju.edu.cn; huminglie@tju.edu.cn).

Abstract: We demonstrate that third-order dispersion (TOD) precompensation accompanied with nonlinear compensation can improve the pulse quality of high energy pulses in fiber chirped-pulse amplification (FCPA) system. The negative TOD fiber is implemented as the precompensation of TOD mismatch, resulting small required B-integral, which benefits the pulse quality. The conclusion is given by analytical study and numerical simulations. Based on this method, we obtain high-energy pulses up to 10.4 μJ. The quality of the dechirped pulse is high and $>$90% of pulse energy is contained in the main pulse. The dechirped pulse duration is $\sim$280 fs, which is nearly the same as the transform-limited pulse of the oscillator. The system also shows a wide tunable range of pulse energy from 5 to 10 μJ with the good pulse quality.

Index Terms: Fiber amplifier, femtosecond laser, high energy.

1. Introduction

Due to the high peak power and short pulse duration, femtosecond laser becomes an irreplaceable tool in scientific and industrial areas progressively [1]. Specifically, femtosecond fiber laser shows great potential for delivering high-power short pulses with outstanding beam quality and compactness [2]. However, because of the small fiber core and long interaction length, femtosecond fiber laser system shows restriction on scaling up the pulse energy due to high nonlinearity [3]. To overcome this limitation, chirped-pulse amplification (CPA) is a common method. By using CPA technique in fiber system, the pulse energy can scale up to mJ-level [4]. For common CPA systems, the grating pair used as stretcher can provide an appreciable pulse stretching ratio and a good match with the grating compressor [5], but precise alignment makes the system complicated and hard to operate, and any misalignment will produce spatial and temporal aberrations. A fiber stretcher can solve this problem instead. However, the TOD of the fiber stretcher cannot be compensated by grating compressor [6], which finally distorts the pulse shape after compression [7].

In order to compensate the residual TOD, two main strategies are implemented: the linear compensation and the nonlinear compensation. For linear compensation, it is common to use negative TOD elements, such as prism pairs [8], grism pairs [9], [10], and Gires–Tournois interferometer mirrors [11]. Recently, the negative TOD fiber (NTF) is well designed [12] and commercialized. It provides positive group velocity dispersion (GVD) and negative TOD, which matches the dispersion of the grating pair. By using this fiber as stretcher, the FCPA system can generate clean and short dechirped pulses [13]. Nevertheless, the β_3/β_2 of NTF is limited by the fiber structure and cannot be very high. Although the dispersion of fiber stretcher well matches that of grating compressor with the help of NTF, the gain narrowing effect will make the dechirped pulse much longer than the seed pulse of the oscillator. As for nonlinear compensation, Wise *et al*. and Shah *et al*. demonstrated that the nonlinear phase shift induced by self-phase modulation (SPM) effect can be used to compensate the residual TOD caused by the mismatch between the fiber stretcher and the grating compressor [14], [15]. However, because the large required nonlinearity will induce uncompensated phase shift after compression and cause the pulse degradation and the relative peak power reduction [16], the TOD that can be compensated by the nonlinear phase shift is not infinite. As a result, the length of the stretcher fiber is limited, which finally restricts the achievable pulse energy of the FCPA system.

In this paper, we use the NTF to control the residual TOD and apply nonlinear amplification in the power amplifier to avoid gain narrowing effect, as well as provide nonlinear phase shift for TOD compensation. With the help of TOD pre-compensation by NTF, the required nonlinear phase shift is reduced significantly, and as a consequence, the pulse quality is much higher than that in a simple nonlinear compensation system. Theoretically, we figure out the relations between the initial TOD, the nonlinearity and the pulse quality. To be more precise, the results of a more practical situation are provided by the numerical simulations. Basing on the theoretical framework, we obtain 280-fs, 10-μJ pulses with high quality, of which $>$90% energy is concentrated in the main pulse, corresponding to $\sim$37-MW peak power.

2. Analysis of the Method

In an FCPA system, the propagation of the pulse is complicated and several important parameters can affect the output laser characteristics. In this contribution, we first give an analytical derivation of the pulse propagation in FCPA system. The method of stationary phase is used here to achieve the transformation between time-domain and frequency-domain [17], [18]. Compared with the large stretching phase, the phase of the seed pulse can be neglected. Therefore, the derivation starts from a zero phase spectrum.

First, we consider a simple stretcher, so the nonlinearity and higher order dispersion are neglected. Consequently, the pulses undergoing GVD and TOD in stretcher can be written as follows [19]:

$$A_{st}(T) = \frac{1}{2\pi}\int d\Omega \exp(-i\Omega T)\exp\left(i\frac{\phi_{st}^{(2)}}{2}\Omega^2 + i\frac{\phi_{st}^{(3)}}{6}\Omega^3\right)\tilde{A}_0(\Omega), \tag{1}$$

where Ω is the difference between the angular frequency and the central angular frequency; T is the retarded frame. $\tilde{A}_0(\Omega)$ refers to slow varying amplitude of the initial spectrum. $\phi_{st}^{(2)}$ and $\phi_{st}^{(3)}$ are the second and third derivative of the stretching phase respectively, i.e. the total amount of GVD and TOD accumulated in fiber stretcher. After stretching, the pulses are amplified in an amplifier which has a spectrally uniform gain and a simple nonlinearity (only SPM). The nonlinearity in the amplifier is presented as B-integral [3]. At last, the pulses are compressed by a grating compressor, with which negative group delay dispersion (GDD) ($\phi_{com}^{(2)}$) and positive TOD ($\phi_{com}^{(3)}$) are added. After the derivation, the expression of the output spectral amplitude can be given by

$$\tilde{A}_{amp}(\Omega) = \exp\left(\frac{gL}{2}\right)\tilde{A}_0(\Omega)\exp\left(i\frac{\phi_{st}^{(2)}+\phi_{com}^{(2)}}{2}\Omega^2 + i\frac{\phi_{st}^{(3)}+\phi_{com}^{(3)}}{6}\Omega^3\right)\exp(iBs(\Omega)) \tag{2}$$

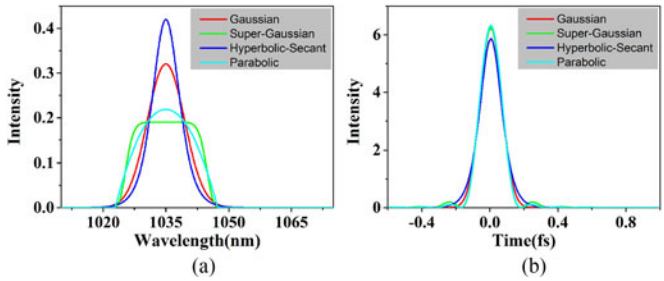

Fig. 1. (a) Initial spectra with equivalent energy. (b) Corresponding TL pulses with same FWHM duration (150 fs).

where g is the gain coefficient, L is the length of amplifier, and $s(\Omega)$ is the initial spectral shape. B refers to the accumulated nonlinear phase shift (i.e., B-integral) caused by SPM effect in the amplifier, which is defined as $B = \gamma L_{eff} \max[|A_{st}(T)|^2]$. For a given stretcher or compressor, the β_3/β_2 is constant, namely, $\phi_{st}^{(3)} = C_{st}\phi_{st}^{(2)}$ and $\phi_{com}^{(3)} = C_{com}\phi_{com}^{(2)}$. So the spectral amplitude after compression can be rewritten as

$$\tilde{A}_{com}(\Omega) = \exp\left(\frac{gL}{2}\right)\tilde{A}_0(\Omega)\exp\left(i\frac{\left(\phi_{st}^{(2)}+\phi_{com}^{(2)}\right)\Omega^2}{2} + i\frac{\left(C_{st}\phi_{st}^{(2)}+C_{com}\phi_{com}^{(2)}\right)\Omega^3}{6}\right)\exp\left(iBs(\Omega)\right). \tag{3}$$

Equation (3) includes the phase induced by the stretching, the compression and the SPM. Based on the method of stationary phase, the intensity profile can be mapped from time-domain to frequency-domain and *vice versa*. Therefore, the temporal-profile-related nonlinear phase shift will be dependent on the spectral shape and described as $Bs(\Omega)$ in (3). Consequently, the compressed temporal pulse quality will be related to the initial spectral shape. To give a general conclusion, we choose several different spectral shapes (as shown in Fig. 1). The pulses with different spectral shapes have identical energy and full-width at half maximum (FWHM) duration of transform-limited (TL) pulse (150 fs). The initial GDD ($\phi_{st}^{(2)}$) of stretcher and C_{com} of compressor are fixed to 2.3 ps^2 and –0.0088 ps respectively, corresponding to the parameters used in the experiment. The maximal peak intensity of the dechirped pulse is found by adjusting GDD ($\phi_{com}^{(2)}$) of compressor.

To assess the pulse quality, the Root-Mean-Square (RMS) duration is applied [19]. As shown in Fig. 2, the RMS duration maps with respect to initial TOD and B-integral of these four initial spectra are different. However, shorter pulses ($\tau_{RMS} < 200$ fs) can be obtained only when the initial TOD is negative and B-integral is small. Especially, RMS duration increases obviously when initial TOD changes from negative to positive, indicating that the accumulation of TOD degrades the pulse quality. The RMS duration also increases with rising B-integral (except for the situation of parabolic spectrum) because of the accumulation of uncompensated nonlinear phase.

However, the RMS duration cannot figure out the detailed structure of the pulse. As depicted in Fig. 1(b), all the pulses are Gaussian-like, so we define a misfit parameter as the misfit between the dechirped pulse profile $|A(t)|^2$ and the Gaussian fit $|A_{fit}(t)|^2$ to evaluate the cleanliness of the pulse:

$$M^2 = \int\left(|A(t)|^2 - |A_{fit}(t)|^2\right)^2 dt \Big/ \int |A(t)|^4 dt \tag{4}$$

Furthermore, the Strehl Ratio [18] is also used here as an important parameter to assess the pulse quality. Fig. 3(a)–(d) and (e)–(h) depict M and Strehl Ratio with respect to initial TOD and B-integral, respectively. For the given B-integral, proper TOD in the system (contains both the initial TOD of the stretching and the TOD of the compression) will compensate with nonlinearity mutually, which leads to better pulse quality and higher Strehl Ratio compared with non-TOD condition [16], but M, as well as Strehl Ratio, deviates from the optimal value with the increasing B-integral. As

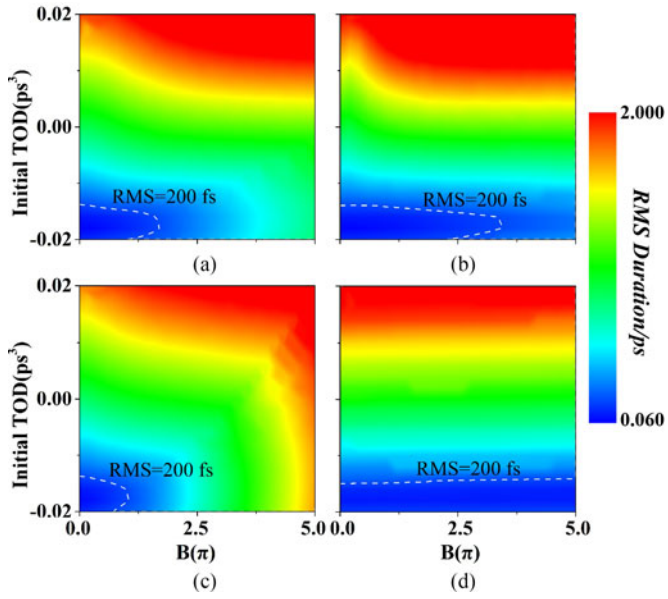

Fig. 2. RMS duration vs initial TOD and B-integral for different spectra. (a) Gaussian. (b) Super-Gaussian. (c) Hyperbolic-Secant. (d) Parabolic. The areas of $\tau_{RMS} < 200$ fs are surrounded by the white dash lines.

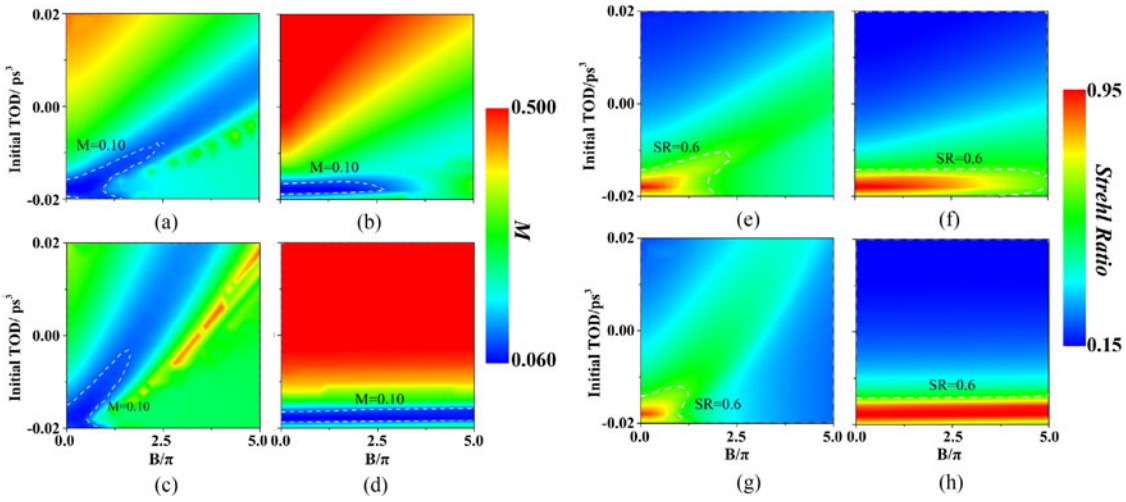

Fig. 3. Misfit parameter and Strehl Ratio maps for different spectra. (a), (e) Gaussian. (b), (f) Super-Gaussian. (c), (g) Hyperbolic-Secant. (d), (h) Parabolic. The areas with M < 0.1 and with SR > 0.6 are marked with white dash lines, respectively.

shown in Fig. 3, analogous to RMS duration evolution, smaller M and higher Strehl Ratio show up in the negative initial TOD region again.

Just comparing these four spectra, parabolic spectrum is an exception. The RMS duration, M and Strehl Ratio nearly do not change with the increasing B-integral [as shown in Figs. 2(d) and 3(d) and (h)]. It is mainly because under this condition the SPM only introduces second-order phase which can be perfectly compensated by the grating pair. Consequently, the parabolic spectrum supports good pulse quality over a wide range of B-integral. Lots of work has been reported on generating high-quality and short pulses with parabolic spectrum, especially the self-similar evolution [20], [21]. However, energy extraction from the self-similar amplifier is limited by Stimulated Raman Scattering

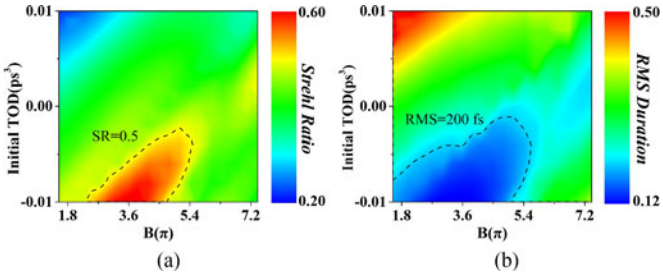

Fig. 4. (a) Strehl Ratio and (b) RMS duration maps in the numerical simulation.

[22] and gain bandwidth [23]. As a result, to deliver higher energy pulses from a fiber system, the most efficiency way is still to use FCPA system in which a very large stretching ratio is essential for high energy. Therefore, the larger B-integral is indispensable to compensate the massive residual TOD caused by the mismatch. Inevitably, due to the accumulation of uncompensated nonlinear phase, the quality of the output pulses will be degraded, and the Strehl Ratio decreases seriously. Fortunately, with a proper negative initial TOD, we can make TOD pre-compensation and reduce the required B-integral to obtain high-quality pulses. With this method, high energy and high pulse quality can be achieved simultaneously in the FCPA system.

To verify the feasibility of this method in a more practical situation, numerical simulations are employed. The numerical model is set based on the experimental setup [depicted in Fig. 5(a)]. Unlike the work in [16], the gain is wavelength dependent, which is derived from [24]. The standard rate and propagation equations for a homogeneously broadened two-level system are utilized, which are solved by the fourth-order Runge-Kutta formula [25], while the Nonlinear Schrödinger Equations (NLSE) in each fiber stage are solved through split-step technique [19]. The simulation begins with an experimentally measured spectrum [depicted in Fig. 5(b)], which is similar to the Super-Gaussian spectrum. Since the AC trace of the dechirped pulse is nearly the same as that of the TL pulse [as shown in Fig. 5(b)], we can simply assume a flat phase for the seed pulse. In the simulation, the GDD of the fiber stretcher is fixed to $2.3\,\mathrm{ps}^2$, while the TOD is changed from $-0.01\,\mathrm{ps}^3$ to $0.01\,\mathrm{ps}^3$. The pump power of the final stage is changed to obtain different B-integral. With the gratings, the pulse is compressed to the shortest FWHM duration, similar to the experimental operation. As shown in Fig. 4, the maps of the Strehl Ratio and RMS duration are not the same as those of Super-Gaussian spectrum discussed before. It is mainly caused by the gain shaping effect. Due to the wavelength-dependent gain, the gain fiber not only provides gain, but also acts as a spectral filter. For a high gain coefficient, the transmission profile of the gain filter is Gaussian-like rather than Super-Gaussian-like [25], which shapes the initial spectrum and pulse and affects the results, but it still shows the same conclusion as before: The negative initial TOD will benefit both pulse quality and Strehl Ratio (as shown in Fig. 4). When the initial TOD is chosen properly, there will be a wide tunable range to achieve high pulse quality (the areas surrounded by the dark dash line, as shown in Fig. 4).

Basing on the theoretical study, we can make sure that in an FCPA system the proper negative TOD accompanied with small B-integral is a good choice to output high-energy pulses with high pulse quality. When extracting high energy from an FCPA system, we can introduce negative TOD to pre-compensate the TOD of grating pair, and hence with only small B-integral the residual TOD can be canceled completely without heavily temporal degradation. Moreover, along with the proper negative TOD, the pulse can maintain its quality over a wider range of B-integral.

3. Experimental Results and Discussion

The schematic of the experimental setup is illustrated in Fig. 5(a). The system is composed of an oscillator, two pulse pickers, a hybrid fiber stretcher, two pre-amplifiers, a power amplifier and

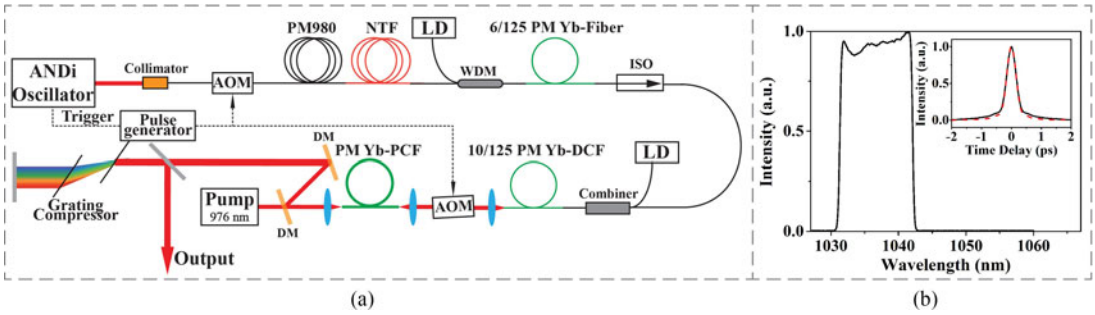

Fig. 5. (a) Setup of the FCPA system. LD, laser diode; WDM, wavelength division multiplexer; ISO, isolator; DM, dichroic mirror; AOM, acoustic-optical modulator; (b) Spectrum and the dechirped auto-correlation (AC) trace of the seed pulse from the oscillator. The red dash line presents the AC trace of the TL pulse. (The pulse duration is ~270 fs.)

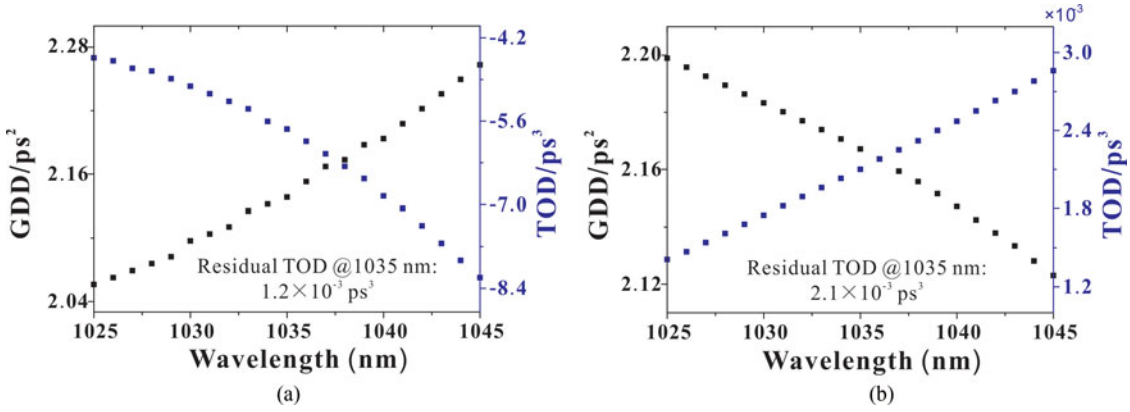

Fig. 6. Dispersion curves of (a) hybrid stretcher and (b) normal stretcher.

a grating compressor. The oscillator is a home-made all-normal-dispersion mode-locked Yb^{3+}-doped fiber laser, which directly generates 100-mW pulse train at 50-MHz repetition rate. The spectrum of the seed pulse is shown in Fig. 5(b), whose bandwidth (FWHM) is ~11 nm centered at 1037 nm. The AC traces of both the dechirped pulse and the corresponding TL pulse are depicted in the inset of Fig. 5(b), which have close pulse duration and pulse shape, The hybrid fiber stretcher consists of 50-m PM980 fiber and 8-m NTF (stretcher fiber, OFS), which offers positive GVD and negative TOD, opposite to those of the compressor. With this hybrid stretcher, the initial amount of TOD is set to about $-0.006\,ps^3$, while the GDD is still as large as $\sim 2.1\,ps^2$ by which the seed pulse can be stretched to ~50 ps. Compared with normal fiber stretcher (the dispersion curves of both stretchers are depicted in Fig. 6), the hybrid stretcher not only provides large GDD, but also alleviates the TOD mismatch. Assuming the distance between the gratings is ~3.7 cm, by which the compressor can afford $\sim -2.1\text{-}ps^2$ GDD, the residual TOD with the hybrid stretcher is $\sim 1.2 \times 10^{-3}\,ps^3$, while that with the normal fiber stretcher is $\sim 2.1 \times 10^{-3}\,ps^3$, almost double that of hybrid stretcher. Consequently, the system shows small net TOD accumulation in the system, and hence small B-integral can compensate the residual TOD. Two AOMs act as pulse pickers and reduce the repetition rate from 50 MHz to 500 kHz.

Accompanied with the increasing pulse energy, the core size of each amplifier stage is increased step by step to maintain a low level of nonlinearity as much as possible. In the first-stage amplifier, highly Yb^{3+}-doped polarization-maintained (PM) single-mode (SM) fiber with 6-μm core diameter (PM-YSF-HI, Nufern) is used to amplify the small signal. Then further amplification is done in the second-stage, whose gain fiber is Yb^{3+}-doped double-cladding PM fiber (PLMA-YDF-10/125-M,

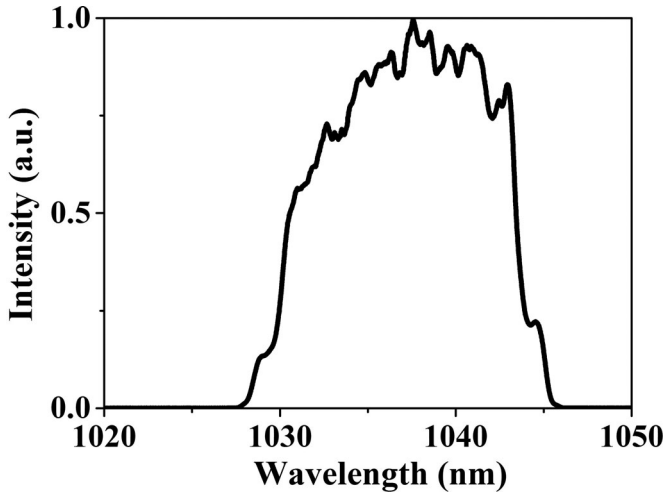

Fig. 7. Spectrum before power amplifier.

Nufern) with a 10-μm core diameter. To keep single-mode operation, the fiber is properly coiled to suppress the high-order modes. Some passive fiber elements used in the system, such as WDM [26], and complex nonlinear effects, such as stimulated Raman scattering and four-wave mixing [15], can introduce spectral modulation, and further the SPM effect can enhance this modulation [27]. As a result, the spectrum before the power amplifier shows modulated structure (as depicted in Fig. 7), and meanwhile it is broadened a little by the SPM. After the second AOM, $\sim$30-mW pulses are coupled into the power amplifier.

The gain fiber of power amplifier is single-polarization double-clad Yb^{3+}-doped large mode area photonic crystal fiber (DC-200-40-PZ-Yb-03, NKT) with 40-μm core diameter. The gain fiber is counter-directionally pumped, in which condition the ASE can be properly suppressed. Since the gain spectrum is related to the fiber length, the gain fiber is set for 1.4 m to match the central wavelength of signal pulse. Both fiber ends are polished to 8° to eliminate parasitic oscillation. The pump and the signal are separated by dichroic mirrors. Then the amplified pulse is compressed by a transmission grating pair with 1600 lines/mm which provides large negative GVD, as well as large positive TOD.

By adjusting the distance between the grating pair, the pulses are compressed to the minimum FWHM duration under each output power. The AC trace and the spectrum of the compressed pulse are recorded at different output powers, according to which the temporal intensity and phase of the pulse can be retrieved by the phase and intensity from correlation and spectrum only (PICASO) algorithm [28]. The retrieved pulses and the spectra under each output power are shown in Fig. 8(a). With increasing output power, the SPM effect is enhanced during amplification, resulting in B-integral increasing. The approximate B-integral can be given by assuming an exponential amplification [29]. In time domain, the rising nonlinear phase shift gradually compensates the third-order phase caused by residual TOD, resulting the enhancement of the pulse quality. On the other hand, the spectral modulation is deepened during the amplification, and the modulation depth increases with the rising B-integral. As the directly output power rises to 7.8 W, the residual TOD and the B-integral ($\sim$4.6 π) are balanced, resulting the highest pulse quality. Fig. 8(b) illustrates that the misfit parameter is lower than 0.1 for varying output power from 5.2 W to 8.6 W, which means that our system can support a wide tunable range of pulse energy to obtain high-quality pulses. Since the spectrum is mapped into time domain for large-chirped pulses, the temporal intensity profile is related to the spectrum, implying that the nonlinear phase shift depends on the spectral profile. Consequently, the spectral modulation can cause the accumulation of irregular nonlinear phase shift during amplification, and finally this uncompensated nonlinear phase shift

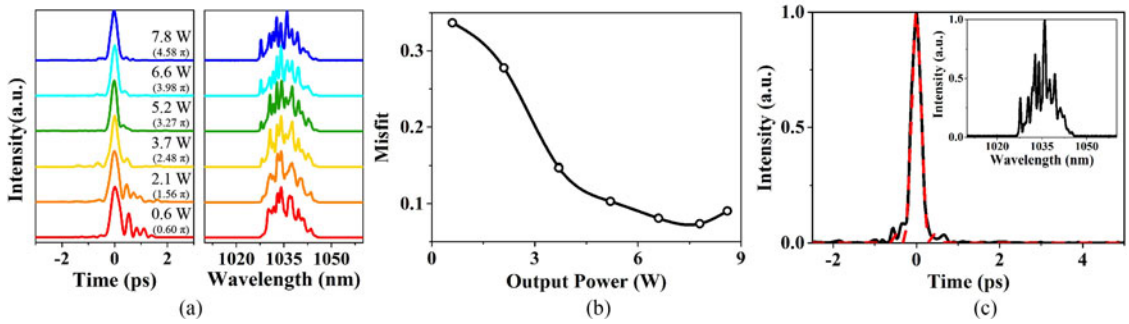

Fig. 8. (a) Retrieved pulse profiles and Spectra of different output powers. (b) Pulse quality with respect to the output power. (c) Retrieved pulse profile and spectrum of the highest pulse energy. Red dash line refers to the TL pulse of the seed from the oscillator.

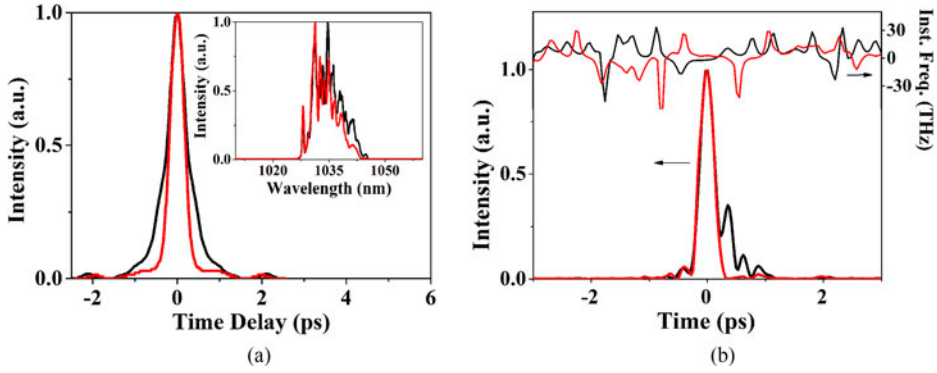

Fig. 9. (a) AC traces and spectra. (b) Retrieved pulses and phase, of hybrid stretcher (red line) and normal fiber stretcher (black line).

will degrade the pulse, especially for high pulse energy. With ~60% compression efficiency, the highest output power after grating pair is 5.2 W, corresponding to 10.4-μJ pulse energy. The FWHM duration of the dechirped pulse is ~280 fs. As shown in Fig. 8(c), the dechirped pulse is nearly the same as the TL pulse of the oscillator. It is because the gain narrowing in the amplifier is compensated by the presence of SPM [30]. The misfit parameter is 0.09, a fairly low level, and over 90% energy is maintained in the main pulse peak. The corresponding peak power is as high as ~37 MW.

As a comparison, we replace the hybrid stretcher with normal fiber stretcher (~100-m PM SMF) which supplies nearly the same GDD but positive TOD on the contrary. The dispersion curves are depicted in Fig. 6(b). With both stretchers, the AC traces and spectra of the compressed pulses are compared at the same output power, i.e. the same B-integral, as is shown in Fig. 8(a). The pump power of the first stage pre-amplifier is adjusted to cover the insertion loss brought in by hybrid stretcher, which causes the small difference between the two spectra [as shown in the inset of Fig. 9(a)]. Based on the AC traces and spectra, the retrieved pulse intensity profile and temporal phase are depicted in Fig. 9(b). Due to the large mismatch between the grating and the normal stretcher, the residual TOD of the system is considerable and cannot be compensated under this small B-integral. As a result, the dechirped pulse shows obvious oscillation, while the main pulses of these two pulses have much better overlap. Since the residual TOD of the system with a normal fiber stretcher is almost twice that of hybrid stretcher, the B-integral that needs to compensate the mismatch will increase a lot, and as a consequence, the large B-integral can cause the pulse degradation.

4. Conclusion

We have demonstrated a method to generate pulses with high quality as well as high energy from the FCPA system theoretically and experimentally. With the help of NTF, we successfully reduce the residual TOD of the system by the TOD pre-compensation, compared with normal FCPA system. During the amplification, small nonlinearity can be used to compensate the residual TOD, which will not accumulate excessive irregular nonlinear phase shift. Due to spectral broadening by SPM, the gain narrowing effect is also canceled. With this method, $>$10-μJ dechirped pulses with high quality are achieved. The main pulse contains $>$90% of total energy. In the experiment, high-quality pulses can be output with varying dechirped pulse energy from 5 μJ to 10 μJ. Due to the enhancement of the spectral modulation by high nonlinearity, the uncompensated nonlinear phase shift will be accumulated and then degrade the pulse quality. We believe that larger negative TOD and larger mode area can support much higher pulse energy, as well as the high pulse quality.

References

[1] M. E. Fermann and I. Hartl, "Ultrafast fiber laser technology," *IEEE J. Sel. Topics Quantum Electron.*, vol. 15, no. 1, pp. 191–206, Jan. 2009.

[2] C. Jauregui, J. Limpert, and A. Tünnermann, "High-power fibre lasers," *Nature Photon.*, vol. 7, no. 11, pp. 861–867, 2013.

[3] M. D. Perry, T. Ditmire, and B. Stuart, "Self-phase modulation in chirped-pulse amplification," *Opt. Lett.*, vol. 19, no. 24, pp. 2149–2151, 1994.

[4] J. Limpert, F. Roser, T. Schreiber, and A. Tunnermann, "High-power ultrafast fiber laser systems," *IEEE J. Sel. Topics Quantum Electron.*, vol. 12, no. 2, pp. 233–244, Mar./Apr. 2006.

[5] D. Strickland and G. Mourou, "Compression of amplified chirped optical pulses," *Opt. Commun.*, vol. 56, no. 3, pp. 219–221, 1985.

[6] P. Maine, D. Strickland, P. Bado, M. Pessot, and G. Mourou, "Generation of ultrahigh peak power pulses by chirped pulse amplification," *IEEE J. Quantum Electron.*, vol. 24, no. 2, pp. 398–403, Feb. 1988.

[7] M. Stern, J. P. Heritage, and E. Chase, "Grating compensation of third-order fiber dispersion," *IEEE J. Quantum Electron.*, vol. 28, no. 12, pp. 2742–2748, Dec. 1992.

[8] S. Kane, J. Squier, J. Rudd, and G. Mourou, "Hybrid grating–prism stretcher–compressor system with cubic phase and wavelength tunability and decreased alignment sensitivity," *Opt. Lett.*, vol. 19, no. 22, pp. 1876–1878, 1994.

[9] S. Kane and J. Squier, "Grating compensation of third-order material dispersion in the normal dispersion regime: Sub-100-fs chirped-pulse amplification using a fiber stretcher and grating-pair compressor," *IEEE J. Quantum Electron.*, vol. 31, no. 11, pp. 2052–2057, Nov. 1995.

[10] N. Forget, V. Crozatier, and P. Tournois, "Transmission bragg-grating grisms for pulse compression," *Appl. Phys. B*, vol. 109, no. 1, pp. 121–125, 2012.

[11] C. Xie *et al.*, "Vector-dispersion compensation and pulse pedestal cancellation in a femtosecond nonlinear amplification fiber laser system," *Opt. Lett.*, vol. 36, no. 21, pp. 4149–4151, 2011.

[12] L. G. Nielsen, D. Jakobsen, K. G. Jespersen, and B. Pálsdóttir, "A stretcher fiber for use in fs chirped pulse Yb amplifiers," *Opt. Exp.*, vol. 18, no. 4, pp. 3768–3773, 2010.

[13] D. Mortag *et al.*, "Sub-200 fs microjoule pulses from a monolithic linear fiber CPA system," *Opt. Commun.*, vol. 285, no. 5, pp. 706–709, 2012.

[14] S. Zhou, L. Kuznetsova, A. Chong, and F. W. Wise, "Compensation of nonlinear phase shifts with third-order dispersion in short-pulse fiber amplifiers," *Opt. Exp.*, vol. 13, no. 13, pp. 4869–4877, 2005.

[15] L. Shah, Z. Liu, I. Hartl, G. Imeshev, G. C. Cho, and M. E. Fermann, "High energy femtosecond Yb cubicon fiber amplifier," *Opt. Exp.*, vol. 13, no. 12, pp. 4717–4722, 2005.

[16] A. Chong, L. Kuznetsova, and F. W. Wise, "Theoretical optimization of nonlinear chirped-pulse fiber amplifiers," *J. Opt. Soc. Amer. B*, vol. 24, no. 8, pp. 1815–1823, 2007.

[17] J. D. Murray, *Asymptotic Analysis*, vol. 48. New York, NY, USA: Springer, 2012.

[18] D. N. Schimpf, E. Seise, J. Limpert, and A. Tünnermann, "Self-phase modulation compensated by positive dispersion in chirped-pulse systems," *Opt. Exp.*, vol. 17, no. 7, pp. 4997–5007, 2009.

[19] G. P. Agrawal, *Nonlinear Fiber Optics*. New York, NY, USA: Academic, 2007.

[20] Y. Deng, C. Chien, B. G. Fidric, and J. D. kafka, "Generation of sub-50 fs pulses from a high-power Yb-doped fiber amplifier," *Opt. Lett.*, vol. 34, no. 22, pp. 3469–3471, 2009.

[21] S. Wang *et al.*, "Self-similar evolution in a short fiber amplifier through nonlinear pulse preshaping," *Opt. Lett.*, vol. 38, no. 3, pp. 296–298, 2013.

[22] D. B. S. Soh, J. Nilsson, and A. B. Grudinin, "Efficient femtosecond pulse generation using a parabolic amplifier combined with a pulse compressor. I. Stimulated Raman-scattering effects," *J. Opt. Soc. Amer. B*, vol. 23, no. 1, pp. 1–9, 2006.

[23] D. B. S. Soh, J. Nilsson, and A. B. Grudinin, "Efficient femtosecond pulse generation using a parabolic amplifier combined with a pulse compressor. II. Finite gain-bandwidth effect," *J. Opt. Soc. Amer. B*, vol. 23, no. 1, pp. 10–19, 2006.

[24] H. M. Pask *et al.*, "Ytterbium-doped silica fiber lasers: Versatile sources for the 1-1.2 μm region," *IEEE J. Sel. Topics Quantum Electron.*, vol. 1, no. 1, pp. 2–13, Apr. 1995.
[25] S. Wang, B. Liu, M. Hu, and C. Wang, "Amplification and bandwidth recovery of chirped super-gaussian pulses by use of gain shaping in ytterbium-doped fiber amplifiers," *J. Lightw. Technol.*, vol. 32, no. 22, pp. 3827–3835, Nov. 2014.
[26] D. Mortag, D. Wandt, U. Morgner, D. Kracht, and J. Neumann, "Sub-80-fs pulses from an all-fiber-integrated dissipative-soliton laser at 1 μm," *Opt. Exp.*, vol. 19, no. 2, pp. 546–551, 2011.
[27] D. N. Schimpf, E. Seise, J. Limpert, and A. Tünnermann, "The impact of spectral modulations on the contrast of pulses of nonlinear chirped-pulse amplification systems," *Opt. Exp.*, vol. 16, no. 14, pp. 10664–10674, 2008.
[28] J. W. Nicholson and W. Rudolph, "Noise sensitivity and accuracy of femtosecond pulse retrieval by phase and intensity from correlation and spectrum only (PICASO)," *J. Opt. Soc. Amer. B*, vol. 19, no. 2, pp. 330–339, 2002.
[29] M. Muller *et al.*, "1 kW 1 mJ eight-channel ultrafast fiber laser," *Opt. Lett.*, vol. 41, no. 15, pp. 3439–3442, 2016.
[30] D. N. Papadopoulos, M. Hanna, F. Druon, and P. Georges, "Compensation of gain narrowing by self-phase modulation in high-energy ultrafast fiber chirped-pulse amplifiers," *IEEE J. Sel. Topics Quantum Electron.*, vol. 15, no. 1, pp. 182–186, Jan. 2009.